



1       **Optical properties and molecular compositions of water-soluble and water-**  
2                   **insoluble brown carbon (BrC) aerosols in Northwest China**

3

4       Jianjun Li<sup>1,2</sup>, Qi Zhang<sup>2,\*</sup>, Gehui Wang<sup>1,3,4,\*</sup>, Jin Li<sup>1</sup>, Can Wu<sup>1,3</sup>, Lang Liu<sup>1</sup>, Jiayuan Wang<sup>1,2</sup>,

5                   Wenqing Jiang<sup>2</sup>, Lijuan Li<sup>1,2</sup>, Kin Fai Ho<sup>1,5</sup>, Junji Cao<sup>1</sup>

6

7       <sup>1</sup> Key Lab of Aerosol Chemistry & Physics, SKLLQG, Institute of Earth Environment, Chinese  
8       Academy of Sciences, Xi'an 710061, China

9       <sup>2</sup> Department of Environmental Toxicology, University of California, Davis, CA 95616, USA

10       <sup>3</sup> Key Laboratory of Geographic Information Science of the Ministry of Education, School of  
11       Geographic Sciences, East China Normal University, Shanghai 200241, China

12       <sup>4</sup> Institute of Eco-Chongming, 3663 N. Zhongshan Rd., Shanghai 200062, China

13       <sup>5</sup> The Jockey Club School of Public Health and Primary Care, The Chinese University of Hong  
14       Kong, Hong Kong, China

15

16

17       \*Corresponding authors:

18       Prof. Qi Zhang

19       Department of Environmental Toxicology, University of California, Davis

20       One Shields Avenue, Davis, CA 95616

21       Phone: 1-530-752-5779

22       Fax: 1-530-752-3394

23       Email: dkwzhang@ucdavis.edu;

24

25       Prof. Gehui Wang

26       School of Geographic Sciences, East China Normal University, Shanghai, China

27       500 Dongchuan Rd., Shanghai 200241, China

28       Phone: 86-21-5434-1193

29       E-mail: ghwang@geo.ecnu.edu.cn.

30



31 **Abstract**

32 Brown carbon (BrC) contributes significantly to aerosol light absorption, thus can affect the earth's  
33 radiation balance and atmospheric photochemical processes. In this study, we examined the light  
34 absorption properties and molecular compositions of water-soluble (WS) and water-insoluble (WI)  
35 BrC in PM<sub>2.5</sub> collected from a rural site in the Guanzhong Basin – a highly polluted region in  
36 Northwest China. Both WS-BrC and WI-BrC showed elevated light absorption coefficients (Abs)  
37 in winter (4-7 times of those in summer) mainly attributed to enhanced emissions from residential  
38 biomass burning (BB) for heating. While the average mass absorption coefficients at 365 nm  
39 (MAC<sub>365</sub>) of WS-BrC were similar between daytime and nighttime in summer (0.99±0.17 and  
40 1.01±0.18 m<sup>2</sup> g<sup>-1</sup>, respectively), the average MAC<sub>365</sub> of WI-BrC was more than a factor of 2 higher  
41 during daytime (2.45±1.14 m<sup>2</sup> g<sup>-1</sup>) than at night (1.18±0.36 m<sup>2</sup> g<sup>-1</sup>). This difference was mainly  
42 attributed to enhanced photochemical formation of WI-BrC species, such as oxygenated polycyclic  
43 aromatic hydrocarbons (OPAHs). In contrast, the MACs of WS-BrC and WI-BrC were generally  
44 similar in winter and both showed little diel differences. The Abs of WS-BrC correlated strongly  
45 with relative humidity, sulfate, and NO<sub>2</sub>, suggesting that aqueous-phase reactions is an important  
46 pathway for secondary BrC formation during the winter season in Northwest China. Nitrophenols  
47 on average contributed 2.44±1.78% of the Abs of WS-BrC in winter, but only 0.12±0.03% in  
48 summer due to faster photodegradation reactions. WS-BrC and WI-BrC were estimated to account  
49 for 0.83±0.23% and 0.53±0.33%, respectively, of the total down-welling solar radiation in the UV  
50 range in summer, and 1.67±0.72% and 2.07±1.24%, respectively, in winter. The total absorption  
51 by BrC in the UV region was about 55-79% relative to the elemental carbon (EC) absorption.

52 **Keywords:** Brown Carbon (BrC); Organic Aerosol; Optical Property; Molecular Composition



54 **1. Introduction**

55 Light-absorbing organic matter, termed as “brown carbon (BrC)”, has been recognized as an  
56 important climate forcer due to its ability to directly interact with both incoming solar radiation  
57 and outgoing terrestrial radiation (Andreae and Gelencser, 2006;Laskin et al., 2015). BrC is a  
58 complex mixture of organic compounds, which collectively show a light absorption profile  
59 increasing exponentially from the visible (Vis) to the ultraviolet (UV) range. Due to the high  
60 abundance of organic aerosol in continental regions, especially in places with intensive  
61 anthropogenic pollution, the contribution of BrC to aerosol absorption in the near-UV range is  
62 potentially significant (Kirillova et al., 2014b;Huang et al., 2018;Yan et al., 2015). For example, a  
63 model study showed that BrC contributes up to  $+0.25 \text{ W m}^{-2}$  of radiative forcing on a planetary  
64 scale, which is approximately 19% of the absorption by anthropogenic aerosols (Feng et al., 2013).  
65 Moreover, the strong absorption of BrC in the UV spectral region can reduce the solar actinic flux,  
66 and subsequently affect atmospheric photochemistry and tropospheric ozone production (Jacobson,  
67 1998;Mohr et al., 2013).

68 A thorough understanding of the sources and transformation processes of BrC in the  
69 atmosphere is important, but it is still lacking. Biomass/biofuel combustion, including forest fires,  
70 and burning of wood and agricultural wastes for residential cooking and heating, has been shown  
71 as a particularly important source of BrC (Washenfelder et al., 2015;Desyaterik et al., 2013;Lin et  
72 al., 2017). BrC can also be emitted directly from coal burning (Yan et al., 2017), and biogenic  
73 release of fungi, plant debris, and humic matter (Rizzo et al., 2013;Rizzo et al., 2011). In addition,  
74 recent studies suggested that secondary BrC can be formed through various reaction pathways,  
75 including photooxidation of aromatic volatile organic compounds (VOCs) (Lin et al., 2015;Liu et



76 al., 2016), reactive uptake of isoprene epoxydiols onto preexisting sulfate aerosols (Lin et al.,  
77 2014), aqueous oxidation of phenolic compounds and  $\alpha$ -dicarbonyls (Chang and Thompson,  
78 2010;Nozière and Esteve, 2005;Smith et al., 2016;Yu et al., 2014;Xu et al., 2018), and reactions  
79 of ammonia or amines with carbonyl compounds in particles or cloud droplets (Nozière et al.,  
80 2007;Laskin et al., 2010;Updyke et al., 2012;Nguyen et al., 2012;De Haan et al., 2018;Powelson  
81 et al., 2014). However, atmospheric oxidation processes may also cause “photobleach” –  
82 photodegradation of BrC into less light-absorbing compounds (Lee et al., 2014;Romonosky et al.,  
83 2015;Sumlin et al., 2017), which may complicate the understanding of BrC in the atmosphere.

84 A common way to quantify the absorption properties of BrC is to measure the absorbance of  
85 aerosol extracts over a wide wavelength range using spectrophotometers. This approach can  
86 differentiate the interference of black carbon (BC) or mineral dust (Hecobian et al., 2010). Most  
87 of the studies use ultrapure water to extract organic substance in the aerosol, and thus measure the  
88 optical properties of water-soluble BrC (WS-BrC) (Wu et al., 2019;Hecobian et al., 2010;Kirillova  
89 et al., 2014b). In addition, some studies analyzed the light absorption of BrC extracted using polar  
90 organic solvents such as methanol or acetone (Liu et al., 2013;Huang et al., 2018;Kim et al., 2016).  
91 Since such extracts contain both water-soluble and water-insoluble chromophores, little  
92 information is available regarding the contribution and formation of water-insoluble BrC (WI-  
93 BrC). However, it is important to understand WI-BrC given the facts that some water-insoluble  
94 organic compounds, such as polycyclic aromatic hydrocarbons and their derivatives, are effective  
95 light absorbers and that the mass absorption of WI-BrC could be even greater than that of the  
96 water-soluble fraction (Chen and Bond, 2010;Huang et al., 2018;Sengupta et al., 2018). Thus, it is  
97 necessary to extract water-soluble and water-insoluble organic components separately, e.g., via



98 using solvents with different polarity in sequence. Combining with measurements of BrC  
99 molecular compositions, the UV-vis absorption properties of the water-soluble and water-insoluble  
100 extracts may help us better understand the sources and formation mechanisms of light-absorbing  
101 compounds in the atmosphere.

102 China has been experiencing serious atmospheric pollution conditions in recent decades, and  
103 both model and field results showed elevated light absorption of BrC in most regions of China  
104 (Huang et al., 2018; Cheng et al., 2011; Yan et al., 2017; Li et al., 2016b) compared to developed  
105 countries such as the U.S. (Hecobian et al., 2010; Washenfelder et al., 2015) and European  
106 countries (Mohr et al., 2013; Teich et al., 2017). However, BrC-related data are scarce in the  
107 Guanzhong Basin (Shen et al., 2017; Huang et al., 2018), which is one of the most polluted regions  
108 in China (van Donkelaar et al., 2010). Here we present measurements of the optical properties of  
109 WS-BrC and WI-BrC in PM<sub>2.5</sub> collected from a rural area of the Guanzhong Basin during winter  
110 and summer seasons. We also measured the concentrations of several BrC compounds as well as  
111 those of organic carbon (OC), elemental carbon (EC), water-soluble OC (WSOC) and inorganic  
112 ions. These data were analyzed to examine the effects of sources emissions, daytime  
113 photochemical oxidation, and aqueous-phase chemistry on WS- and WI-BrC components in  
114 different seasons.

## 115 **2. Experimental section**

### 116 **2.1 Sample collection**

117 The sampling was conducted at a small village (namely Lincun, 34°44' N and 109°32' E, 354m  
118 a.s.l.) ~ 40 km northeast to Xi'an, the capital of Shaanxi Province (Figure S1). The sampling site  
119 is located in the central part of Guanzhong Basin with no obvious point source of air pollutants in



120 the surrounding areas. PM<sub>2.5</sub> samples were collected twice a day (~8 am to 20 pm and ~20 pm to  
121 8 am) onto prebaked (450 °C, 6-8 hr) quartz fiber filters (Whatman, QM-A, USA) during Aug. 3-  
122 23, 2016 and Jan. 20-Feb. 1, 2017 using a TISCH Environmental (USA) PM<sub>2.5</sub> high volume (1.13  
123 m<sup>3</sup> min<sup>-1</sup>) sampler. Field blank samples were also collected by mounting blank filters onto the  
124 sampler for about 15 min without pumping any air. After sampling, the sample filters were  
125 immediately sealed in aluminum foil bags, and then stored in a freezer (-5 °C) prior to analysis.  
126 Meteorological conditions, and concentrations of O<sub>3</sub> and NO<sub>2</sub> during this studied period are  
127 presented in Figure 1.

## 128 **2.2 Filter extraction and absorption spectra analysis**

129 For each PM<sub>2.5</sub> sample, a portion of the filter (~13.384 cm<sup>2</sup>) was first extracted in 8 ml of  
130 Milli-Q water (18.2 MΩ) through 30 min of sonication at ~0°C. The water extract was then filtered  
131 via vacuum filtration with a 25mm diameter 5 μm pore hydrophobic PTFE membrane filter (Merck  
132 Millipore Ltd, Mitex™ Membrane Filters, USA). Afterwards, the insoluble PM components  
133 collected on the PTFE membrane filter and remained on the sample filter were rinsed with 2 ml  
134 Milli-Q water, air dried, and then extracted via sonication in 8 ml pure acetonitrile (ACN)  
135 (Honeywell Burdick & Jackson, LC/MS Grade, USA). The acetonitrile extract was filtered via a  
136 13 mm diameter 0.45 μm pore syringe filter (PALL, Bulk Acrodisc®, PTFE Membrane Filters,  
137 USA). The light absorption spectra of the water and the acetonitrile extracts were measured  
138 between 190 nm to 820 nm by a diode-array spectrophotometer (Hewlett Packard 8452A, USA)  
139 using quartz cuvettes with 1 cm length path. Field blank filters were extracted and measured in the  
140 same manner as the samples. Data presented in this study were corrected for the field blanks (<10%  
141 relative to field samples).



## 142 2.3 Chemical Analysis

143 OC and EC were analyzed using DRI Carbon Analyzer (Model 2001, USA). Another piece  
144 of the filter sample (~8.6 cm<sup>2</sup>) was extracted with Milli-Q water (18.2MΩ), and filtered through  
145 a PTFE syringe filter. Then the water-extract was analyzed for water-soluble inorganic ions  
146 (SO<sub>4</sub><sup>2-</sup>, NO<sub>3</sub><sup>-</sup>, NH<sub>4</sub><sup>+</sup>, Cl<sup>-</sup>, F<sup>-</sup>, Ca<sup>2+</sup>, K<sup>+</sup>, Na<sup>+</sup> and Mg<sup>2+</sup>) using a Metrohm Ion Chromatography  
147 (Metrohm 940, Switzerland) and WSOC using a Shimadzu TOC analyzer (TOC-L CPH, Japan)  
148 and. Concentrations of individual molecules, including levoglucosan, parent-PAHs, Oxygenated-  
149 PAHs (OPAHs), nitrophenols, and isoprene and α-/β-pinene derived products, were measured  
150 using GC/EI-MS (Agilent 7890A-5975C, USA) calibrated by authentic standards. More details  
151 on these measurements can be found in previous publications (Li et al., 2014).

## 152 2.4 Data Interpretation

153 In this study, water-insoluble OC (WIOC) was calculated by the difference between OC and  
154 WSOC:

$$155 M_{WIOC} = M_{OC} - M_{WSOC} \quad (1)$$

156 where  $M_{WIOC}$ ,  $M_{OC}$ , and  $M_{WSOC}$  correspond to the mass concentration (in  $\mu\text{gC m}^{-3}$ ) of WIOC,  
157 OC, and WSOC, respectively, in the air.

158 The absorption coefficient of WS-BrC ( $Abs_{\lambda, WS-BrC}$ ,  $\text{Mm}^{-1}$ ) or WI-BrC ( $Abs_{\lambda, WI-BrC}$ ,  $\text{Mm}^{-1}$ )  
159 at a given wavelength ( $\lambda$ ) is determined from the UV-vis spectrum of the water extract (Hecobian  
160 et al., 2010; Laskin et al., 2015)

$$161 Abs_{\lambda} = (A_{\lambda} - A_{700}) \times \frac{V_{solvent}}{V_a \times l} \times \ln(10) \times 100 \quad (2)$$

162 where  $A_{\lambda}$  is the absorbance of the water ( $A_{\lambda, WS-BrC}$ ) or ACN ( $A_{\lambda, WI-BrC}$ ) extract at  $\lambda$ ,  $V_{solvent}$  (ml)  
163 is the volume of solvent (water or ACN) used to extract the filter (8 mL), and  $V_a$  ( $\text{m}^3$ ) is the air



164 volume passed through the filter punch.  $l$  (cm) is the optical length of the quartz cuvettes used for  
165 UV-vis measurement and  $\ln(10)$  is used to convert the logbase-10 (provided by the  
166 spectrophotometer) to natural logarithm. 100 is for unit conversion.  $A_{700}$  (absorbance at the  
167 wavelength of 700 nm) is subtracted to minimize the interference of baseline shift. The mass  
168 absorption coefficient of WS-BrC ( $MAC_{\lambda, WS-BrC}$ ,  $m^2 g^{-1}$ ) or WI-BrC ( $MAC_{\lambda, WI-BrC}$ ,  $m^2 g^{-1}$ ) at  
169 wavelength of  $\lambda$  is calculated using eq (3)

$$170 \quad MAC_{\lambda} = \frac{Abs_{\lambda}}{M} \quad (3)$$

171 Note that since it is possible that not all the WI-BrC was extracted into ACN, the  $Abs_{\lambda, WI-BrC}$  and  
172  $MAC_{\lambda, WI-BrC}$  reported in this study are likely the lower bound values. Nevertheless, the  
173 underestimation is probably insignificant since Chen and Bond (Chen and Bond, 2010) reported  
174 that >92% of BrC was extractable by organic solvents (methanol or acetone).

175 The wavelength dependence for BrC absorption is fit with a power law equation:

$$176 \quad Abs_{\lambda} = K \times \lambda^{-AAE} \quad (4)$$

177 where  $K$  is a constant and AAE stands for absorption Ångström exponent. In this study, the AAE  
178 for a given sample is calculated through the linear regression of  $\log(Abs_{\lambda})$  against  $\log \lambda$  between  
179 300–450 nm. This wavelength range is chosen because the fits of all the samples in this study are  
180 better than  $r^2=0.99$ . Note that slightly higher AAE values (by up to 10%) are obtained using a  
181 wider wavelength range (e.g., 300-550 nm; Figure S2).

182 The fraction of solar irradiance absorbed by particulate BrC at a given wavelength  $\lambda$  is  
183 estimated following the Beer–Lambert’s law:

$$184 \quad \frac{I_0 - I}{I_0}(\lambda) = 1 - e^{-b_{ap, \lambda, x} \times h_{ABL}} \quad (5)$$

185 where  $x$  denotes WS-BrC or WI-BrC,  $h_{ABL}$  is the atmospheric boundary layer height (assuming





186 1200 m in summer and 600 m in winter) according to the assumption that the ground  
187 measurement results are representative of the average values in the whole atmospheric boundary  
188 layer (ABL) (Kirchstetter et al., 2004; Kirillova et al., 2014a), and  $b_{ap,\lambda,x}$  corresponds to the  
189 absorption coefficient ( $b_{ap, m^{-1}}$ ) of WS-BrC or WI-BrC at wavelength of  $\lambda$ . Previous studies  
190 showed that the light absorption coefficient of particulate BrC ( $b_{ap,\lambda,BrC}$ ) is around 0.7–2.0 times  
191 of that from bulk solution ( $Abs_{\lambda,WS-BrC \text{ or } WI-BrC}$ ) (Liu et al., 2013; Sun et al., 2007). Here, a  
192 conversion factor of 1.3 is applied based on a Mie theory calculation of aerosols in Xi'an (~ 40  
193 km away from the sampling site) (Wu, 2018).  $I_0$  denotes the incident solar radiance in the form  
194 of either actinic flux (in quanta  $s^{-1} cm^{-2} nm^{-1}$ ) or irradiance (in  $W m^{-2} nm^{-1}$ ), which were obtained  
195 using the TUV Quick Calculator ([http://cprm.acom.ucar.edu/Models/TUV/Interactive\\_TUV/](http://cprm.acom.ucar.edu/Models/TUV/Interactive_TUV/)).  
196 ( $I_0-I$ ) denotes the direct absorption of solar actinic flux or irradiance by BrC.

### 197 3. Results and Discussion

#### 198 3.1 Optical absorption characteristics of WS-BrC and WI-BrC

199 The average absorption spectra of WS-BrC and WI-BrC ( $\lambda = 300-700$  nm) during daytime  
200 and nighttime in different seasons are shown in Figure 2a & b. The absorption Ångström  
201 exponents for both WS-BrC ( $AAE_{WS-BrC}$ ) and WI-BrC ( $AAE_{WI-BrC}$ ) are generally higher than 5,  
202 verifying the contribution of BrC to aerosol absorptivity in the region. The average  $AAE_{WS-BrC}$   
203 are similar between summer ( $5.43 \pm 0.41$ ) and winter ( $5.11 \pm 0.53$ ). Huang et al. (2014) and Shen et  
204 al. (2017) reported comparable  $AAE_{WS-BrC}$  values (5.3–5.7) with no significant seasonal change  
205 at urban sites of Xi'an, suggesting common characteristics of BrC on a regional scale in the  
206 Guanzhong Basin of China. Comparable AAE values were reported for WS-BrC in Switzerland  
207 (3.8–5.1) (Moschos et al., 2018) and Nepal (4.2–5.6) (Wu et al., 2019; Kirillova et al., 2016), but



208 higher  $AAE_{WS-BrC}$  were found in Southeastern US ( $7 \pm 1$ ) (Hecobian et al., 2010), Los Angeles  
209 Basin ( $7.6 \pm 0.5$ ) (Zhang et al., 2013), Korea ( $5.84-9.17$ ) (Kim et al., 2016), and Beijing ( $7.0-7.5$ )  
210 (Cheng et al., 2011).

211 The  $AAE_{WI-BrC}$  shows more obvious seasonal variations with a higher average value in  
212 winter ( $6.04 \pm 0.22$ ) than in summer ( $5.01 \pm 0.58$ ). This difference suggests that the chemical  
213 composition of WI-BrC might be more different in different seasons, due to variations in the  
214 sources and atmospheric formation and aging processes of light absorbing hydrophobic  
215 compounds.

216 The light absorption properties of WS-BrC and WI-BrC present obvious seasonal variations  
217 (Figure 2). The average ( $\pm 1\sigma$ ) Abs and MAC values of BrC at 365 nm (i.e.,  $Abs_{365,WS-BrC}$ ,  
218  $Abs_{365,WI-BrC}$ ,  $MAC_{365,WS-BrC}$ , and  $MAC_{365,WI-BrC}$ ) during daytime and nighttime in winter and  
219 summer are summarized in Table 1. 365 nm is chosen to avoid interferences from inorganic  
220 compounds (e.g., nitrate and nitrite) and to be consistent with previous studies (Hecobian et al.,  
221 2010; Huang et al., 2018). On average,  $Abs_{365,WS-BrC}$  is significantly higher than  $Abs_{365,WI-BrC}$  in  
222 summer ( $5.00 \pm 1.28 \text{ Mm}^{-1}$  vs.  $2.95 \pm 1.94 \text{ Mm}^{-1}$ ) but the values are comparable in winter ( $19.6 \pm 8.3$   
223  $\text{Mm}^{-1}$  vs.  $21.9 \pm 13.5 \text{ Mm}^{-1}$ ). The substantially higher BrC absorptions in winter correspond to a  
224 much higher organic aerosol concentration – WSOC and WIOC concentrations in winter are on  
225 average 4.2 and 14 times of the concentrations in summer (Table 1). Elevated OA (organic  
226 aerosols) concentration during winter is due to a combination of lower ABL height and enhanced  
227 primary emissions (e.g., from residential heating) in the cold season. It is worth noting that the  
228 wavelength-dependent Abs of WS-BrC shows a minor tip at about 360 nm in both seasons  
229 (Figure 2), which may be related to the contribution of some specific chromophores. For



230 example, Lin et al. (2015) reported that some nitrogen-containing organic compounds (such as  
231 picric acid or nitrophenol) have a maximum absorption at wavelength of ~360 nm.

232 The MACs of WS-BrC are comparable between the two seasons (Figure 2c & d), with the  
233 average  $MAC_{365,WS-BrC}$  being  $1.00 (\pm 0.18) \text{ m}^2 \text{ g}^{-1}$  in summer and  $0.93 (\pm 0.25) \text{ m}^2 \text{ g}^{-1}$  in winter  
234 (Table 1). As summarized in Table 2, the  $MAC_{365,WS-BrC}$  measured in this study, i.e., at a rural  
235 site in the Guanzhong Basin of China, is comparable to or lower than the values observed in  
236 Asian cities such Xi'an (Huang et al., 2018), Beijing (Cheng et al., 2011), Seoul (Kim et al.,  
237 2016) and New Delhi (Kirillova et al., 2014b). However, significantly lower  $MAC_{365,WS-BrC}$   
238 values were observed in the US, including Los Angeles Basin (Zhang et al., 2013), Southeastern  
239 US (Hecobian et al., 2010), and Atlanta (Liu et al., 2013).

240 In winter, the average  $MAC_{365,WI-BrC}$  ( $0.95 \pm 0.32 \text{ m}^2 \text{ g}^{-1}$ ) is comparable to  $MAC_{365,WS-BrC}$   
241 ( $0.93 \pm 0.25 \text{ m}^2 \text{ g}^{-1}$ ; Table 1). However, in summer the  $MAC_{365,WI-BrC}$  is significantly higher than  
242  $MAC_{365,WS-BrC}$  ( $1.82 \pm 1.06$  vs.  $1.00 \pm 0.18 \text{ m}^2 \text{ g}^{-1}$ ), indicating a relatively stronger light absorption  
243 capability of hydrophobic chromophores than hydrophilic chromophores. Further, the fact that  
244 the summertime  $MAC_{365,WI-BrC}$  is nearly double the wintertime  $MAC_{365,WI-BrC}$  suggests that more  
245 light absorbing molecules are formed in the warm season.

246 Figure 2 compares the wavelength-dependent light absorptivity (i.e.,  $Abs_{\lambda}$  and  $MAC_{\lambda}$ ) of  
247 WS-BrC and WI-BrC between day and night in summer and winter. Higher  $Abs_{\lambda,WS-BrC}$  and  
248  $Abs_{\lambda,WI-BrC}$  occurred during daytime in summer but during nighttime in winter. The  $MAC_{\lambda}$  of  
249 WS-BrC are overall similar between daytime and nighttime in both seasons. However, the  $MAC_{\lambda}$   
250 of WI-BrC show a significant daytime increase in summer over the whole wavelength range of  
251 300-700 nm (Figure 2c). The day-night change of BrC light absorptivity can be viewed more



252 obviously in Figure 1e and 1f, where the temporal variations of the  $Abs_{365}$  and  $MAC_{365}$  of WS-  
253 BrC and WI-BrC during summer 2016 (Aug. 3-23) and winter 2017 (Jan. 20 -Feb. 1) are  
254 presented. The highest day/night ratio of  $MAC_{365,WIOc}$  reached 3.8 in summer and the average  
255 daytime  $MAC_{365,WI-BrC}$  in summer ( $2.45 \pm 1.14 \text{ m}^2 \text{ g}^{-1}$ ) is more than twice the value during  
256 nighttime ( $1.18 \pm 0.36 \text{ m}^2 \text{ g}^{-1}$ ; Table 1). A possible reason for this observation is that there are  
257 additional sources of WI-BrC during summer daytime in this rural region, such as secondary  
258 formation of hydrophobic light absorbing compounds.

259 Figure 3 and 4 present the cross-correlations of  $Abs_{365,WS-BrC}$  and  $Abs_{365,WI-BrC}$  with major  
260 chemical components (e.g., WSOC, WSIC, and sulfate) and molecular tracer species in summer  
261 and winter, respectively. In winter,  $Abs_{365,WS-BrC}$  correlates strongly with WSOC concentration  
262 ( $r^2=0.80$ ), so does  $Abs_{365,WI-BrC}$  with WIOC ( $r^2=0.76$ ). However, their relationships in summer are  
263 much weaker, especially for the correlation between  $Abs_{365,WI-BrC}$  and WIOC ( $r^2=0.50$ ).  
264 Considering that secondary OA (SOA) are mainly comprised of water-soluble compounds, such  
265 as polyalcohols/polyacids and phenols (Kondo et al., 2007), the much higher WSOC/OC ratio in  
266 summer ( $0.75 \pm 0.07$ ) compared to winter ( $0.50 \pm 0.09$ ) confirms more prevalent SOA formation in  
267 summer associated with higher air temperature and stronger solar radiation. Formation of  
268 secondary organic chromophores may lead to a more complex composition of BrC in summer.  
269 More evidences on secondary BrC formation are provided in the subsequent sections.

270 Numerous studies reported that biomass burning is a dominant source of BrC in the  
271 atmosphere (Desyaterik et al., 2013; Washenfelder et al., 2015). In the current study,  
272 levoglucosan – a key tracer for biomass burning emissions (Simoneit, 2002) – was determined.  
273 As shown in Figure 3 and 4, levoglucosan correlates well with WSOC and WIOC in both



274 summer and winter ( $r^2=0.45-0.77$ ), suggesting that biomass burning is an important source of OA  
275 in the rural region of Guanzhong Basin. For most of the periods in this study, the  $MAC_{365,WS-BrC}$   
276 and  $MAC_{365,WI-BrC}$  values are within the range of MAC of biomass burning aerosols (e.g.,  
277 1.3–1.8 for corn stalk (Li et al., 2016a), 1.37 for rice straw (Park and Yu, 2016), ~1.9 for BB  
278 smoke particles (Lin et al., 2017)). Also,  $Abs_{365,WI-BrC}$  in both summer and winter correlate well  
279 with levoglucosan ( $r^2=0.74$  and  $0.62$ , respectively), demonstrating an important contribution of  
280 biomass burning to WI-BrC despite the fact that levoglucosan itself is water soluble. The  
281 relationships between the  $Abs_{365,WS-BrC}$  and levoglucosan are much weaker ( $r^2=0.40$  and  $0.45$  in  
282 summer and winter, respectively), suggesting more complex sources of WS-BrC in the region.

### 283 3.2 Molecular characterization of BrC aerosols

284 Five categories of molecular tracer compounds, i.e., parent-polycyclic aromatic  
285 hydrocarbons (parent-PAHs), oxygenated-PAHs (OPAHs), nitrophenols, isoprene-derived  
286 products ( $SOA_i$ ), and  $\alpha$ -/ $\beta$ -pinene-derived products ( $SOA_p$ ), were determined by the GC-EIMS  
287 technique to investigate the formation pathways of BrC in this study. Their average  
288 concentrations as well as daytime and nighttime differences are summarized in Table 1, and the  
289 temporal variation profiles of the sum concentrations of each category, together with  
290 levoglucosan time series, are presented in Figure S3.

291 PAHs and their derived compounds are important BrC chromophores, since the large  
292 conjugated polycyclic structures are strongly light-absorbing in the near-UV range (Samburova  
293 et al., 2016;Huang et al., 2018). A total number of 14 parent PAHs and 5 OPAHs (Table S1)  
294 were determined in this study. Parent-PAHs are unsubstituted PAHs mainly emitted directly  
295 from incomplete combustions of coal, biofuel, gasoline or other materials whereas OPAHs can



296 be emitted directly from combustion sources or formed from photochemical oxidation of the  
297 parent-PAHs. The time trends of parent-PAHs and OPAHs are highly similar in both seasons ( $r^2$   
298 = 0.90 and 0.98 in summer and winter, respectively, Figure 3 and 4), suggesting that they have  
299 common combustion sources. In addition, both parent-PAHs and OPAHs presented good  
300 correlations with levoglucosan, particularly in winter ( $r^2 = 0.69$  and  $0.73$ , respectively; Figure 4),  
301 indicating that that biomass burning is an important contributor to air particulate PAHs in the  
302 region. PAHs, as well as levoglucosan, are elevated during nighttime in winter, corresponding to  
303 enhanced biomass burning emissions from heating-related activities as well as reduced boundary  
304 layer height at night. In contrast, the average daytime concentrations of parent-PAHs ( $11.6 \pm 5.7$   
305  $\text{ng m}^{-3}$ ) and levoglucosan ( $142 \pm 89 \text{ ng m}^{-3}$ ) in summer are about 1.95 and 2.58 times,  
306 respectively, of the values at night (Table 1). The daytime enhancement of OPAHs  
307 concentrations in summer is even more pronounced with an average day/night ratio of  $\sim 4.6$  and  
308 as high as 9.8 for individual OPAH species (e.g., 6H-henzo(cd)pyrene-6-one; Figure S4). Both  
309 parent-PAHs and OPAHs, which are hydrophobic thus mainly exist as WIOC, demonstrate a  
310 good linear relationship with  $\text{Abs}_{365, \text{WI-BrC}}$  in both winter and summer ( $r^2 = 0.49$ - $0.83$ , Figure 3  
311 and 3). However, the good correlation between OPAHs and  $\text{Abs}_{365, \text{WI-BrC}}$  in summer appears to  
312 be mainly driven by daytime production, as the correlation coefficient ( $r^2$ ) is 0.72 for the daytime  
313 data but is  $< 0.1$  for the nighttime data (Figure S5a). These results suggest that photochemical  
314 formation of light-absorption compounds is an important source of BrC during summer in the  
315 Guanzhong Basin.

316 We estimated the potential contribution of parent-PAHs and OPAHs to the light absorption  
317 of WI-BrC using a method reported in Samburova et al. (2016). Details on the method are



318 presented in the Supplementary Information (SI). Table S2 summarizes the solar-spectrum-  
319 weighed mass absorption coefficients for PAHs ( $MAC_{PAH,av}$ ) used in the calculation. As shown  
320 in Figure 5, the contribution of parent-PAHs to solar-spectrum-weighted absorption coefficient of  
321 WI-BrC varies between 0.55% - 0.66% with slight diurnal or season variations (Table S2).  
322 However, the contribution of OPAHs clearly shows higher daytime values, especially in  
323 summer. The average contribution of OPAHs to the solar-spectrum-weighted absorption  
324 coefficient of WI-BrC in summer is  $0.51 \pm 0.28\%$  during daytime and  $0.34 \pm 0.19\%$  during  
325 nighttime. These results indicate that more secondary water-insoluble aromatic chromophores  
326 were produced via photochemical oxidation during summertime in the rural region.

327 Nitrophenols were identified as one of the most important light-absorbing compounds in  
328 particles and cloud water influenced by BB emission in China (Desyaterik et al., 2013). These  
329 compounds can be either directly emitted from burning of biomass (Xie et al., 2019) or formed in  
330 the atmosphere through gas phase and aqueous phase reactions of aromatic precursors including  
331 benz[a]pyrene (Lu et al., 2011), naphthalene (Kitanovski et al., 2014), catechol and guaiacol  
332 (Ofner et al., 2011), and toluene (Liu et al., 2015) in the presence of  $NO_x$ . In this study, only a  
333 few nitrophenol compounds were detected in PM (Table S1) and their average ( $\pm 1\sigma$ )  
334 concentration is  $0.94 (\pm 0.26) \text{ ng m}^{-3}$  in summer and  $72.6 (\pm 63.7) \text{ ng m}^{-3}$  in winter. The  
335 wintertime concentrations of nitrophenols measured in the current study are comparable to those  
336 detected in Shanghai (Li et al., 2016b), Mt. Tai in the Shandong province of China (Desyaterik et  
337 al., 2013), and Ljubljana of Slovenia (Kitanovski et al., 2012), but the summertime  
338 concentrations observed are more comparable to those detected in the Los Angeles Basin of the  
339 U.S. (Zhang et al., 2013). The substantially lower concentration of nitrophenols in summer may



340 be related to rapid photodegradation in the atmosphere. Indeed, according to a laboratory study  
341 conducted by Zhao et al. (2015) the timescale for photo-bleaching of nitrophenols can be an hour  
342 or less. Furthermore, as shown in Figure S5b, during wintertime, when low temperature and  
343 weak solar irradiation suppress photodegradation process, nitrophenols concentration anti-  
344 correlates with O<sub>3</sub> mixing ratio in a nonlinear manner ( $r^2=0.60$ ). On average, nitrophenols in  
345 winter present 2.5 times higher concentration during nighttime than during daytime whereas the  
346 nighttime concentrations of levoglucosan and PAHs are only slightly higher than the daytime  
347 concentrations (by 11% and 33%, respectively; Table 1). Levoglucosan and PAHs are less  
348 photochemically reactive than nitrophenols. These results confirm that nitrophenols, and other  
349 photoreactive BrC compounds, may undergo significant atmospheric degradation during  
350 summertime.

351 Both summertime and wintertime  $\text{Abs}_{365, \text{WS-BrC}}$  correlate well with the concentrations of  
352 nitrophenols ( $r^2=0.51-0.72$ , Figure S5c & d), suggesting an important contribution of nitrated  
353 aromatic compounds to light absorption of WS-BrC in the study area. Using the MAC of  
354 individual nitrophenol reported in Zhang et al. (2013), we calculated that the contributions of  
355 nitrophenols to aerosol light absorption are 6.5-27 times higher than their mass contributions to  
356 WSOC and that the fractions are much higher in winter ( $2.44 \pm 1.78\%$ ) than in summer  
357 ( $0.12 \pm 0.03\%$ ; Table S3). In addition, due to a significantly higher abundance of nitrophenols  
358 during nighttime in winter, their fractional contribution to aerosol absorption is on average 2.5  
359 times higher than during the day ( $3.47 \pm 2.03\%$  vs.  $1.41 \pm 0.29\%$ ).

360 On a global scale, biogenic VOCs, mostly consisting of isoprene and monoterpenes, are  
361 nearly an order of magnitude more abundant than anthropogenic VOCs (Guenther et al., 2006),





362 and their secondary products are estimated to be a predominant contributor to global SOA  
363 burden (Heald et al., 2008). Recent studies (Lin et al., 2014; Nakayama et al., 2015; Nakayama et  
364 al., 2012) showed that a large amount of biogenic SOA compounds are light absorptive. Some  
365 tracers of SOA formed from isoprene (SOA<sub>i</sub>) and  $\alpha$ -/ $\beta$ -pinene (SOA<sub>p</sub>) oxidation were measured  
366 in the summertime samples (Table S1), and their temporal variations are shown in Figure S3. No  
367 biogenic SOA tracer species were detectable in the winter samples in this study. Similar results  
368 were obtained in our previous study in the Mt. Hua of the Guanzhong Basin (Li, 2011). These  
369 findings are consistent with low emissions of biogenic VOCs and low oxidation rates in this  
370 region during cold seasons. The average concentrations of SOA<sub>i</sub> and SOA<sub>p</sub> tracers in summer are  
371  $18.6 \pm 9.7$  and  $22.0 \pm 6.7$  ng m<sup>-3</sup>, respectively. Neither SOA<sub>i</sub> tracers nor SOA<sub>p</sub> tracers showed  
372 significant correlations with the absorption coefficient of WSOC or WSIC, suggesting a low  
373 contribution of biogenic SOA to aerosol light absorption in the region. In addition, compared to  
374 the MAC values observed in this study, the MACs of biogenic SOA reported in literature are  
375 much lower, on average by nearly an order of magnitude (Laskin et al., 2015), which further  
376 support an insignificant contribution of biogenic sources to BrC in this region. This finding is  
377 consistent with the fact that the Guanzhong Basin is a highly polluted region, where the major  
378 emission sources of organic aerosols are anthropogenic.

### 379 **3.3 Variation of BrC during extreme haze events in winter**

380 In recent years, extreme haze events with very high PM<sub>2.5</sub> concentrations (up to 500-600  $\mu$ g  
381 m<sup>-3</sup>) and low visibility (lower than 1 km) occurred frequently during wintertime in China (Huang  
382 et al., 2014). In this study, an extreme haze event occurred during Jan. 21-26 when PM<sub>2.5</sub>  
383 concentration at the rural site increased continuously from  $\sim 100$   $\mu$ g m<sup>-3</sup> to 430  $\mu$ g m<sup>-3</sup> and



384 visibility decreased from >10 km to ~1.4 km (Figure 1b & d). Similar to most haze events  
385 occurred in Northeast China, this event was associated with stagnant meteorological condition  
386 with low wind speed (<1 km s<sup>-1</sup>) which promotes the accumulation of pollutants. In addition,  
387 secondary inorganic aerosol species, e.g., SO<sub>4</sub><sup>2-</sup>, NO<sub>3</sub><sup>-</sup> and NH<sub>4</sub><sup>+</sup>, increased sharply (Figure 1d),  
388 which indicates secondary aerosol formation was enhanced during the haze event despite the low  
389 solar irradiance and low O<sub>3</sub> concentration (e.g., 2 ~ 40 μg m<sup>-3</sup>; Figure 1c) conditions. Recent  
390 studies by Wang et al. (2016) and Cheng et al. (2016) reported dramatic increases of secondary  
391 inorganic components, mainly sulfate, nitrate and ammonium (SNA), during haze periods in  
392 China and attributed the increases to enhanced aqueous reactions under high relative humidity  
393 (RH) conditions with NO<sub>2</sub> being an important oxidant. Moreover, Huang et al. (2014) observed  
394 that SOA also increased obviously during haze periods in winter. Indeed, as shown in Figure 4,  
395 SO<sub>4</sub><sup>2-</sup> correlates well with RH (r<sup>2</sup>=0.64) and NO<sub>2</sub> (r<sup>2</sup>=0.56) in winter. In addition, Abs<sub>365,WS-BrC</sub>,  
396 which increases continuously during the haze period with a peak value at 43.3 Mm<sup>-1</sup> (Figure 1e),  
397 correlates well with RH (r<sup>2</sup>=0.65), sulfate (r<sup>2</sup>=0.84) and NO<sub>2</sub> (r<sup>2</sup>=0.70) (Figure 4). These results  
398 suggest that aqueous oxidation has played a role in the formation of WS-BrC. This finding is  
399 consistent with previous studies which have shown that aqueous reactions can be an important  
400 pathway of BrC formation in the atmosphere (Laskin et al., 2015). In contrast, a slowly  
401 decreasing trend of MAC<sub>365,WIOC</sub> is observed during the haze period, suggesting that some of the  
402 water-insoluble BrC species were oxidized to form water-soluble chromophores, possibly  
403 through aqueous-phase reactions.

404 It is worthwhile to mention that Jan. 27, 2017 was the Chinese New Year's Eve and a large  
405 amount of fireworks were set off for celebration. During this night, the MAC<sub>365,WS-BrC</sub> (1.81)



406 increased to about 2 times of its average value in winter, while OC, EC, WSOC and WIOC as  
407 well as SNA were actually 25%-51% lower than their wintertime average concentrations (Figure  
408 1d). Meanwhile, metal ions which are abundant in fireworks (Wu et al., 2018;Jiang et al., 2015),  
409 such as  $K^+$ ,  $Mg^{2+}$ ,  $Ca^{2+}$ , increased substantially during the night as well (Figure S6). These  
410 results indicate that the increase of  $MAC_{365,WSOC}$  during the Chinese New Year's Eve is likely  
411 mainly contributed by metal-containing light-absorbing compounds emitted from fireworks  
412 (Laskin et al., 2015;Tran et al., 2017).

### 413 **3.4 Estimation of direct absorption of solar radiation by BrC**

414 Since the light absorption of BrC is mainly in the UV spectral region, an important concern  
415 is that BrC can reduce the solar actinic flux and thus affect atmospheric photochemistry and  
416 tropospheric ozone production (Jacobson, 1998;Mohr et al., 2013). In this study, the direct  
417 absorptions of solar radiation by both WS-BrC and WI-BrC are estimated using Eq 7. Figure S7  
418 presents the incident solar irradiance and actinic flux spectra determined for the region under  
419 midday summer (Aug. 10, 2016 13:00 pm Beijing (BJ) time) and winter (Jan. 25, 2017 13:00 pm  
420 BJ time) conditions. Note that the local time at Guanzhong is ~ 1 hour later than the BJ time.

421 Table 3 presents a summary of the calculated direct solar absorptions of BrC. In summer,  
422 the direct attenuation of actinic flux by WS-BrC and WI-BrC are estimated at  
423  $1.55 \times 10^{14} \pm 0.43 \times 10^{14}$  and  $1.03 \times 10^{14} \pm 0.64 \times 10^{14}$  quanta  $s^{-1} cm^{-2}$ , respectively, in the UV range  
424 (300-400 nm), which account for  $0.83 \pm 0.23\%$  and  $0.53 \pm 0.33\%$ , respectively, of the total down-  
425 welling radiation. In winter, the direct absorptions by BrC are higher with WS-BrC and WI-BrC  
426 on average account for  $1.67 \pm 0.72\%$  and  $2.07 \pm 1.24\%$ , respectively, of the total down-welling  
427 radiation in the UV range. These results suggest that BrC may have a significant influence on



428 atmospheric photochemistry in the UV range. In the visible spectral region (400 - 700 nm), the  
429 contributions of WS-BrC and WI-BrC to the total down-welling radiation are negligible –  
430  $0.10\pm 0.03\%$  and  $0.07\pm 0.05\%$  in summer, and  $0.15\pm 0.06\%$  and  $0.15\pm 0.08\%$  in winter,  
431 respectively.

432 Another concern of BrC is that they can absorb solar irradiance to influence tropospheric  
433 temperature in a similar way as black carbon (BC) or elemental carbon (EC) (Feng et al.,  
434 2013; Laskin et al., 2015). In our study, the direct absorption of solar irradiance by WS-BrC and  
435 WI-BrC are estimated at  $0.51\pm 0.14$  and  $0.34\pm 0.21$   $\text{W m}^{-2}$  in summer, and  $0.57\pm 0.25$  and  
436  $0.68\pm 0.41$   $\text{W m}^{-2}$  in winter in the UV range. To evaluate the contribution of BrC to total aerosol  
437 absorption, we also estimated the direct absorption of EC based on the Carbon Analyzer data  
438 according to the method described by Kirillova et al. (2014b) and Kirchstetter and Thatcher  
439 (2012) (see SI). The estimated contributions of light absorption of BrC relative to EC are shown  
440 in Table 3. In the visible region, the contribution is estimated at  $10.0\pm 3.52\%$  in summer and  
441  $4.99\pm 1.23\%$  in winter for WS-BrC, and  $6.19\pm 2.42\%$  and  $4.51\pm 1.44\%$ , respectively, for WI-BrC.  
442 However, in the UV range, the fractions increase to  $49.3\pm 14.5\%$  in summer and  $25.9\pm 5.47\%$  in  
443 winter for WS-BrC,  $29.4\pm 11.0\%$  and  $29.0\pm 10.4\%$  for WI-BrC, which are within the range of the  
444 values reported in other regions in China (Huang et al., 2018), India (Kirillova et al., 2014b), and  
445 Korea (Kirillova et al., 2014a). On the other hand, the direct light absorption of WI-BrC  
446 represents a substantive contribution to that of total BrC in this study, which is about 40% in  
447 summer and more than 50% in winter in both UV and visible range, emphasizing the important  
448 role that WI-BrC likely plays in atmospheric chemistry and the Earth's climate system,  
449 especially in China.



#### 450 4. Summary and Conclusion

451 Both WS-BrC and WI-BrC showed elevated Abs in winter (4-7 times higher than those in  
452 summer), corresponding to much higher concentrations of WSOC and WIOC due to a  
453 combination of lower ABL height and enhanced primary emissions (e.g., from residential  
454 heating) in the cold season. No significant differences were found for the daytime and nighttime  
455 MACs of WS-BrC in summer, or for the MACs of WS-BrC and WI-BrC in winter. However, the  
456 average daytime  $MAC_{365,WI-BrC}$  was more than twice the nighttime value in summer. We found  
457 that the average daytime concentrations of both parent-PAHs and levoglucosan in summer were  
458 around 2 times of the values at night and the daytime OPAHs concentration was more than 4  
459 times of the nighttime value. Moreover, OPAHs and  $Abs_{365,WI-BrC}$  correlated well during daytime  
460 ( $r^2=0.72$ ) in summer but not during nighttime ( $r^2<0.1$ ). These results demonstrated that  
461 photochemical formation of BrC and enhanced BB emissions (e.g., from cooking) contributed to  
462 the higher daytime MACs in summer. In winter, the Abs of WS-BrC correlated strongly with  
463 relative humidity, sulfate, and  $NO_2$ , suggesting that aqueous-phase reactions played an important  
464 role in the formation of secondary BrC.  $Abs_{365,WS-BrC}$  correlated well with the concentrations of  
465 nitrophenols in both seasons, suggesting an important contribution of nitrated aromatic  
466 compounds to light absorption of WS-BrC. However, this contribution is much lower in summer  
467 due to faster photodegradation reactions of these compounds. WS-BrC and WI-BrC were  
468 estimated to account for  $0.83\pm 0.23\%$  and  $0.53\pm 0.33\%$ , respectively, of the total down-welling  
469 solar radiation in the UV range in summer, and  $1.67\pm 0.72\%$  and  $2.07\pm 1.24\%$ , respectively, in  
470 winter. The substantive contribution of WI-BrC to total BrC absorption (~40% in summer  
471 and >50% in winter) emphasize the important role that WI-BrC likely plays in atmospheric



472 chemistry and the Earth's climate system.

473

474

475

#### 476 **Author Contributions**

477 J.J. Li, Q. Zhang, G.H. Wang, K.F. Ho, and J.J. Cao designed the experiment. J.J. Li, G.H. Wang,  
478 and K.F. Ho arranged the sample collection. J. Li, L. Liu and C. Wu collected the samples. J.J.  
479 Li, J. Li, J.Y. Wang, W.Q. Jiang, and L.J. Li analyzed the samples. J.J. Li, Q. Zhang, and G.H.  
480 Wang performed the data interpretation. J.J. Li, Q. Zhang, and G.H. Wang wrote the paper.

481

#### 482 **Acknowledgements**

483 This work was financially supported by the program from National Nature Science Foundation  
484 of China (No. 41773117, 91644102, 41977332, 91543116). The authors gratefully acknowledge  
485 National Center for Atmospheric Research for the provision of the solar actinic flux and  
486 irradiance data (TUV Quick Calculator,  
487 [http://cprm.acom.ucar.edu/Models/TUV/Interactive\\_TUV/](http://cprm.acom.ucar.edu/Models/TUV/Interactive_TUV/)) used in this publication.

488

489

#### 490 **References**

- 491 Andreae, M. O., and Gelencser, A.: Black carbon or brown carbon? The nature of light-absorbing carbonaceous  
492 aerosols, *Atmos. Chem. Phys.*, 6, 3131-3148, 10.5194/acp-6-3131-2006, 2006.
- 493 Chang, J. L., and Thompson, J. E.: Characterization of colored products formed during irradiation of aqueous  
494 solutions containing H<sub>2</sub>O<sub>2</sub> and phenolic compounds, *Atmos. Environ.*, 44, 541-551,  
495 10.1016/j.atmosenv.2009.10.042, 2010.
- 496 Chen, Y., and Bond, T. C.: Light absorption by organic carbon from wood combustion, *Atmos. Chem. Phys.*, 10,  
497 1773-1787, 10.5194/acp-10-1773-2010, 2010.
- 498 Cheng, Y., He, K. B., Zheng, M., Duan, F. K., Du, Z. Y., Ma, Y. L., Tan, J. H., Yang, F. M., Liu, J. M., Zhang, X. L.,  
499 Weber, R. J., Bergin, M. H., and Russell, A. G.: Mass absorption efficiency of elemental carbon and water-  
500 soluble organic carbon in Beijing, China, *Atmos. Chem. Phys.*, 11, 11497-11510, 10.5194/acp-11-11497-2011,  
501 2011.
- 502 Cheng, Y., Zheng, G., Wei, C., Mu, Q., Zheng, B., Wang, Z., Gao, M., Zhang, Q., He, K., Carmichael, G., Pöschl,  
503 U., and Su, H.: Reactive nitrogen chemistry in aerosol water as a source of sulfate during haze events in China,  
504 *Science Advances*, 2, 10.1126/sciadv.1601530, 10.1126/sciadv.1601530, 2016.
- 505 De Haan, D. O., Tapavicza, E., Riva, M., Cui, T. Q., Surratt, J. D., Smith, A. C., Jordan, M. C., Nilakantan, S.,  
506 Almodovar, M., Stewart, T. N., de Loera, A., De Haan, A. C., Cazaunau, M., Gratien, A., Pangu, E., and



- 507 Doussin, J. F.: Nitrogen-Containing, Light-Absorbing Oligomers Produced in Aerosol Particles Exposed to  
508 Methylglyoxal, Photolysis, and Cloud Cycling, *Environ. Sci. Technol.*, 52, 4061-4071,  
509 10.1021/acs.est.7b06105, 2018.
- 510 Desyaterik, Y., Sun, Y., Shen, X., Lee, T., Wang, X., Wang, T., and Collett Jr., J. L.: Speciation of “brown” carbon in  
511 cloud water impacted by agricultural biomass burning in eastern China, *J. Geophys. Res.-Atmos.*, 118, 7389-  
512 7399, doi:10.1002/jgrd.50561, 2013.
- 513 Feng, Y., Ramanathan, V., and Kotamarthi, V. R.: Brown carbon: a significant atmospheric absorber of solar  
514 radiation?, *Atmos. Chem. Phys.*, 13, 8607-8621, 10.5194/acp-13-8607-2013, 2013.
- 515 Guenther, A., Karl, T., Harley, P., Wiedinmyer, C., Palmer, P. I., and Geron, C.: Estimates of global terrestrial  
516 isoprene emissions using MEGAN (Model of Emissions of Gases and Aerosols from Nature), *Atmos. Chem.*  
517 *Phys.*, 6, 3181-3210, 2006.
- 518 Heald, C. L., Henze, D. K., Horowitz, L. W., Feddesma, J., Lamarque, J. F., Guenther, A., Hess, P. G., Vitt, F.,  
519 Seinfeld, J. H., Goldstein, A. H., and Fung, I.: Predicted change in global secondary organic aerosol  
520 concentrations in response to future climate, emissions, and land use change, *J. Geophys. Res.-Atmos.*, 113,  
521 doi: 10.1029/2007jd009092, 10.1029/2007jd009092, 2008.
- 522 Hecobian, A., Zhang, X., Zheng, M., Frank, N., Edgerton, E. S., and Weber, R. J.: Water-Soluble Organic Aerosol  
523 material and the light-absorption characteristics of aqueous extracts measured over the Southeastern United  
524 States, *Atmos. Chem. Phys.*, 10, 5965-5977, 10.5194/acp-10-5965-2010, 2010.
- 525 Huang, R.-J., Zhang, Y., Bozzetti, C., Ho, K.-F., Cao, J.-J., Han, Y., Daellenbach, K. R., Slowik, J. G., Platt, S. M.,  
526 Canonaco, F., Zotter, P., Wolf, R., Pieber, S. M., Bruns, E. A., Crippa, M., Ciarelli, G., Piazzalunga, A.,  
527 Schwikowski, M., Abbaszade, G., Schnelle-Kreis, J., Zimmermann, R., An, Z., Szidat, S., Baltensperger, U., El  
528 Haddad, I., and Prevot, A. S. H.: High secondary aerosol contribution to particulate pollution during haze  
529 events in China, *Nature*, 514, 218-222, 10.1038/nature13774, 2014.
- 530 Huang, R.-J., Yang, L., Cao, J., Chen, Y., Chen, Q., Li, Y., Duan, J., Zhu, C., Dai, W., Wang, K., Lin, C., Ni, H.,  
531 Corbin, J. C., Wu, Y., Zhang, R., Tie, X., Hoffmann, T., O’Dowd, C., and Dusek, U.: Brown Carbon Aerosol in  
532 Urban Xi’an, Northwest China: The Composition and Light Absorption Properties, *Environ. Sci. Technol.*, 52,  
533 6825-6833, 10.1021/acs.est.8b02386, 2018.
- 534 Jacobson, M. Z.: Studying the effects of aerosols on vertical photolysis rate coefficient and temperature profiles over  
535 an urban airshed, *J. Geophys. Res.-Atmos.*, 103, 10593-10604, 10.1029/98jd00287, 1998.
- 536 Jiang, Q., Sun, Y. L., Wang, Z., and Yin, Y.: Aerosol composition and sources during the Chinese Spring Festival:  
537 fireworks, secondary aerosol, and holiday effects, *Atmos. Chem. Phys.*, 15, 6023-6034, 10.5194/acp-15-6023-  
538 2015, 2015.
- 539 Kim, H., Kim, J. Y., Jin, H. C., Lee, J. Y., and Lee, S. P.: Seasonal variations in the light-absorbing properties of  
540 water-soluble and insoluble organic aerosols in Seoul, Korea, *Atmos. Environ.*, 129, 234-242,  
541 <https://doi.org/10.1016/j.atmosenv.2016.01.042>, 2016.
- 542 Kirchstetter, T. W., Novakov, T., and Hobbs, P. V.: Evidence that the spectral dependence of light absorption by  
543 aerosols is affected by organic carbon, *J. Geophys. Res.-Atmos.*, 109, doi:10.1029/2004JD004999,  
544 10.1029/2004jd004999, 2004.
- 545 Kirchstetter, T. W., and Thatcher, T. L.: Contribution of organic carbon to wood smoke particulate matter absorption  
546 of solar radiation, *Atmos. Chem. Phys.*, 12, 6067-6072, 10.5194/acp-12-6067-2012, 2012.
- 547 Kirillova, E. N., Andersson, A., Han, J., Lee, M., and Gustafsson, Ö.: Sources and light absorption of water-soluble  
548 organic carbon aerosols in the outflow from northern China, *Atmos. Chem. Phys.*, 14, 1413-1422, 10.5194/acp-  
549 14-1413-2014, 2014a.
- 550 Kirillova, E. N., Andersson, A., Tiwari, S., Srivastava, A. K., Bisht, D. S., and Gustafsson, Ö.: Water-soluble organic



- 551 carbon aerosols during a full New Delhi winter: Isotope-based source apportionment and optical properties, *J.*  
552 *Geophys. Res.-Atmos.*, 119, 3476-3485, 10.1002/2013jd020041, 2014b.
- 553 Kirillova, E. N., Marinoni, A., Bonasoni, P., Vuillermoz, E., Facchini, M. C., Fuzzi, S., and Decesari, S.: Light  
554 absorption properties of brown carbon in the high Himalayas, *J. Geophys. Res.-Atmos.*, 121, 9621-9639,  
555 10.1002/2016jd025030, 2016.
- 556 Kitanovski, Z., Grgić, I., Vermeylen, R., Claeys, M., and Maenhaut, W.: Liquid chromatography tandem mass  
557 spectrometry method for characterization of monoaromatic nitro-compounds in atmospheric particulate matter,  
558 *Journal of Chromatography A*, 1268, 35-43, <https://doi.org/10.1016/j.chroma.2012.10.021>, 2012.
- 559 Kitanovski, Z., Čusak, A., Grgić, I., and Claeys, M.: Chemical characterization of the main products formed through  
560 aqueous-phase photolysis of guaiacol, *Atmos. Meas. Tech.*, 7, 2457-2470, 10.5194/amt-7-2457-2014, 2014.
- 561 Kondo, Y., Miyazaki, Y., Takegawa, N., Miyakawa, T., Weber, R. J., Jimenez, J. L., Zhang, Q., and Worsnop, D. R.:  
562 Oxygenated and water-soluble organic aerosols in Tokyo, *Journal of Geophysical Research*, 112, doi:  
563 10.1029/2006jd007056, 10.1029/2006jd007056, 2007.
- 564 Laskin, A., Laskin, J., and Nizkorodov, S. A.: Chemistry of Atmospheric Brown Carbon, *Chemical reviews*, 4335-  
565 4382, 10.1021/cr5006167, 2015.
- 566 Laskin, J., Laskin, A., Roach, P. J., Slysz, G. W., Anderson, G. A., Nizkorodov, S. A., Bones, D. L., and Nguyen, L.  
567 Q.: High-Resolution Desorption Electrospray Ionization Mass Spectrometry for Chemical Characterization of  
568 Organic Aerosols, *Analytical Chemistry*, 82, 2048-2058, 10.1021/ac902801f, 2010.
- 569 Lee, H. J., Aiona, P. K., Laskin, A., Laskin, J., and Nizkorodov, S. A.: Effect of Solar Radiation on the Optical  
570 Properties and Molecular Composition of Laboratory Proxies of Atmospheric Brown Carbon, *Environ. Sci.*  
571 *Technol.*, 48, 10217-10226, 10.1021/es502515r, 2014.
- 572 Li, J., Wang, G., Aggarwal, S. G., Huang, Y., Ren, Y., Zhou, B., Singh, K., Gupta, P. K., Cao, J., and Zhang, R.:  
573 Comparison of abundances, compositions and sources of elements, inorganic ions and organic compounds in  
574 atmospheric aerosols from Xi'an and New Delhi, two megacities in China and India, *Science of The Total*  
575 *Environment*, 476-477, 485-495, <http://dx.doi.org/10.1016/j.scitotenv.2014.01.011>, 2014.
- 576 Li, J. J.: Chemical Composition, Size distribution and Source Apportionment of Atmospheric Aerosols at an Alpine  
577 Site in Guanzhong Plain, China (in Chinese), Ph. D, Xi'an Jiaotong University, Xi'an, 124 pp., 2011.
- 578 Li, X., Chen, Y., and Bond, T. C.: Light absorption of organic aerosol from pyrolysis of corn stalk, *Atmos. Environ.*,  
579 144, 249-256, <https://doi.org/10.1016/j.atmosenv.2016.09.006>, 2016a.
- 580 Li, X., Jiang, L., Hoa, L. P., Lyu, Y., Xu, T. T., Yang, X., Iinuma, Y., Chen, J. M., and Herrmann, H.: Size distribution  
581 of particle-phase sugar and nitrophenol tracers during severe urban haze episodes in Shanghai, *Atmos.*  
582 *Environ.*, 145, 115-127, 10.1016/j.atmosenv.2016.09.030, 2016b.
- 583 Lin, P., Liu, J., Shilling, J. E., Kathmann, S. M., Laskin, J., and Laskin, A.: Molecular characterization of brown  
584 carbon (BrC) chromophores in secondary organic aerosol generated from photo-oxidation of toluene, *Phys*  
585 *Chem Chem Phys*, 17, 23312-23325, 10.1039/c5cp02563j, 2015.
- 586 Lin, P., Bluvshstein, N., Rudich, Y., Nizkorodov, S. A., Laskin, J., and Laskin, A.: Molecular Chemistry of  
587 Atmospheric Brown Carbon Inferred from a Nationwide Biomass Burning Event, *Environ Sci Technol*, 51,  
588 11561-11570, 10.1021/acs.est.7b02276, 2017.
- 589 Lin, Y.-H., Budisulistiorini, S. H., Chu, K., Siejack, R. A., Zhang, H., Riva, M., Zhang, Z., Gold, A., Kautzman, K.  
590 E., and Surratt, J. D.: Light-Absorbing Oligomer Formation in Secondary Organic Aerosol from Reactive  
591 Uptake of Isoprene Epoxydiols, *Environ. Sci. Technol.*, 48, 12012-12021, 10.1021/es503142b, 2014.
- 592 Liu, J., Bergin, M., Guo, H., King, L., Kotra, N., Edgerton, E., and Weber, R. J.: Size-resolved measurements of  
593 brown carbon in water and methanol extracts and estimates of their contribution to ambient fine-particle light  
594 absorption, *Atmos. Chem. Phys.*, 13, 12389-12404, 10.5194/acp-13-12389-2013, 2013.





- 595 Liu, J., Lin, P., Laskin, A., Laskin, J., Kathmann, S. M., Wise, M., Caylor, R., Imholt, F., Selimovic, V., and Shilling,  
596 J. E.: Optical properties and aging of light-absorbing secondary organic aerosol, *Atmos. Chem. Phys.*, 16,  
597 12815-12827, 10.5194/acp-16-12815-2016, 2016.
- 598 Liu, P. F., Abdelmalki, N., Hung, H. M., Wang, Y., Brune, W. H., and Martin, S. T.: Ultraviolet and visible complex  
599 refractive indices of secondary organic material produced by photooxidation of the aromatic compounds  
600 toluene and m-xylene, *Atmos. Chem. Phys.*, 15, 1435-1446, 10.5194/acp-15-1435-2015, 2015.
- 601 Lu, J. W., Flores, J. M., Lavi, A., Abo-Riziq, A., and Rudich, Y.: Changes in the optical properties of  
602 benzo[a]pyrene-coated aerosols upon heterogeneous reactions with NO<sub>2</sub> and NO<sub>3</sub>, *Physical Chemistry  
603 Chemical Physics*, 13, 6484-6492, 10.1039/C0CP02114H, 2011.
- 604 Mohr, C., Lopez-Hilfiker, F. D., Zotter, P., Prévôt, A. S. H., Xu, L., Ng, N. L., Herndon, S. C., Williams, L. R.,  
605 Franklin, J. P., Zahniser, M. S., Worsnop, D. R., Knighton, W. B., Aiken, A. C., Gorkowski, K. J., Dubey, M.  
606 K., Allan, J. D., and Thornton, J. A.: Contribution of Nitrated Phenols to Wood Burning Brown Carbon Light  
607 Absorption in Detling, United Kingdom during Winter Time, *Environ. Sci. Technol.*, 47, 6316-6324,  
608 10.1021/es400683v, 2013.
- 609 Moschos, V., Kumar, N. K., Daellenbach, K. R., Baltensperger, U., Prévôt, A. S. H., and El Haddad, I.: Source  
610 Apportionment of Brown Carbon Absorption by Coupling Ultraviolet-Visible Spectroscopy with Aerosol Mass  
611 Spectrometry, *Environmental Science & Technology Letters*, 5, 302-308, 10.1021/acs.estlett.8b00118, 2018.
- 612 Nakayama, T., Sato, K., Matsumi, Y., Imamura, T., Yamazaki, A., and Uchiyama, A.: Wavelength Dependence of  
613 Refractive Index of Secondary Organic Aerosols Generated during the Ozonolysis and Photooxidation of  
614  $\alpha$ -Pinene, *SOLA*, 8, 119-123, 10.2151/sola.2012-030, 2012.
- 615 Nakayama, T., Sato, K., Tsuge, M., Imamura, T., and Matsumi, Y.: Complex refractive index of secondary organic  
616 aerosol generated from isoprene/NO<sub>x</sub> photooxidation in the presence and absence of SO<sub>2</sub>, *J. Geophys. Res.-  
617 Atmos.*, 120, 7777-7787, 10.1002/2015jd023522, 2015.
- 618 Nguyen, T. B., Lee, P. B., Updyke, K. M., Bones, D. L., Laskin, J., Laskin, A., and Nizkorodov, S. A.: Formation of  
619 nitrogen- and sulfur-containing light-absorbing compounds accelerated by evaporation of water from secondary  
620 organic aerosols, *J. Geophys. Res.-Atmos.*, 117, 14, 10.1029/2011jd016944, 2012.
- 621 Nozière, B., and Esteve, W.: Organic reactions increasing the absorption index of atmospheric sulfuric acid aerosols,  
622 *Geophysical Research Letters*, 32, doi:10.1029/2004GL021942, 10.1029/2004gl021942, 2005.
- 623 Nozière, B., Dziedzic, P., and Córdoba, A.: Formation of secondary light-absorbing “fulvic-like” oligomers: A  
624 common process in aqueous and ionic atmospheric particles?, *Geophysical Research Letters*, 34,  
625 doi:10.1029/2007GL031300, 10.1029/2007gl031300, 2007.
- 626 Ofner, J., Krüger, H. U., Grothe, H., Schmitt-Kopplin, P., Whitmore, K., and Zetzsch, C.: Physico-chemical  
627 characterization of SOA derived from catechol and guaiacol &ndash; a model substance for the aromatic  
628 fraction of atmospheric HULIS, *Atmos. Chem. Phys.*, 11, 1-15, 10.5194/acp-11-1-2011, 2011.
- 629 Park, S. S., and Yu, J.: Chemical and light absorption properties of humic-like substances from biomass burning  
630 emissions under controlled combustion experiments, *Atmos. Environ.*, 136, 114-122,  
631 <https://doi.org/10.1016/j.atmosenv.2016.04.022>, 2016.
- 632 Powelson, M. H., Espelien, B. M., Hawkins, L. N., Galloway, M. M., and De Haan, D. O.: Brown Carbon Formation  
633 by Aqueous-Phase Carbonyl Compound Reactions with Amines and Ammonium Sulfate, *Environ. Sci.  
634 Technol.*, 48, 985-993, 10.1021/es4038325, 2014.
- 635 Rizzo, L. V., Correia, A. L., Artaxo, P., Procópio, A. S., and Andreae, M. O.: Spectral dependence of aerosol light  
636 absorption over the Amazon Basin, *Atmos. Chem. Phys.*, 11, 8899-8912, 10.5194/acp-11-8899-2011, 2011.
- 637 Rizzo, L. V., Artaxo, P., Müller, T., Wiedensohler, A., Paixão, M., Cirino, G. G., Arana, A., Swietlicki, E., Roldin, P.,  
638 Fors, E. O., Wiedemann, K. T., Leal, L. S. M., and Kulmala, M.: Long term measurements of aerosol optical



- 639 properties at a primary forest site in Amazonia, *Atmos. Chem. Phys.*, 13, 2391-2413, 10.5194/acp-13-2391-  
640 2013, 2013.
- 641 Romonosky, D. E., Laskin, A., Laskin, J., and Nizkorodov, S. A.: High-Resolution Mass Spectrometry and  
642 Molecular Characterization of Aqueous Photochemistry Products of Common Types of Secondary Organic  
643 Aerosols, *The Journal of Physical Chemistry A*, 119, 2594-2606, 10.1021/jp509476r, 2015.
- 644 Samburova, V., Connolly, J., Gyawali, M., Yatavelli, R. L. N., Watts, A. C., Chakrabarty, R. K., Zielinska, B.,  
645 Moosmüller, H., and Khlystov, A.: Polycyclic aromatic hydrocarbons in biomass-burning emissions and their  
646 contribution to light absorption and aerosol toxicity, *Science of The Total Environment*, 568, 391-401,  
647 <https://doi.org/10.1016/j.scitotenv.2016.06.026>, 2016.
- 648 Sengupta, D., Samburova, V., Bhattarai, C., Kirillova, E., Mazzoleni, L., Iaukea-Lum, M., Watts, A., Moosmüller,  
649 H., and Khlystov, A.: Light absorption by polar and non-polar aerosol compounds from laboratory biomass  
650 combustion, *Atmos. Chem. Phys.*, 18, 10849-10867, 10.5194/acp-18-10849-2018, 2018.
- 651 Shen, Z., Zhang, Q., Cao, J., Zhang, L., Lei, Y., Huang, Y., Huang, R. J., Gao, J., Zhao, Z., Zhu, C., Yin, X., Zheng,  
652 C., Xu, H., and Liu, S.: Optical properties and possible sources of brown carbon in PM 2.5 over Xi'an, China,  
653 *Atmos. Environ.*, 150, 322-330, 10.1016/j.atmosenv.2016.11.024, 2017.
- 654 Simoneit, B. R. T.: Biomass burning - A review of organic tracers for smoke from incomplete combustion, *Applied  
655 Geochemistry*, 17, 129-162, 2002.
- 656 Smith, J. D., Kinney, H., and Anastasio, C.: Phenolic carbonyls undergo rapid aqueous photodegradation to form  
657 low-volatility, light-absorbing products, *Atmos. Environ.*, 126, 36-44, 10.1016/j.atmosenv.2015.11.035, 2016.
- 658 Sumlin, B. J., Pandey, A., Walker, M. J., Pattison, R. S., Williams, B. J., and Chakrabarty, R. K.: Atmospheric  
659 Photooxidation Diminishes Light Absorption by Primary Brown Carbon Aerosol from Biomass Burning,  
660 *Environmental Science & Technology Letters*, 4, 540-545, 10.1021/acs.estlett.7b00393, 2017.
- 661 Sun, H., Biedermann, L., and Bond, T. C.: Color of brown carbon: A model for ultraviolet and visible light  
662 absorption by organic carbon aerosol, *Geophysical Research Letters*, 34, doi: 10.1029/2007gl029797,  
663 10.1029/2007gl029797, 2007.
- 664 Teich, M., van Pinxteren, D., Wang, M., Kecorius, S., Wang, Z., Müller, T., Močnik, G., and Herrmann, H.:  
665 Contributions of nitrated aromatic compounds to the light absorption of water-soluble and particulate brown  
666 carbon in different atmospheric environments in Germany and China, *Atmos. Chem. Phys.*, 17, 1653-1672,  
667 10.5194/acp-17-1653-2017, 2017.
- 668 Tran, A., Williams, G., Younus, S., Ali, N. N., Blair, S. L., Nizkorodov, S. A., and Al-Abadleh, H. A.: Efficient  
669 Formation of Light-Absorbing Polymeric Nanoparticles from the Reaction of Soluble Fe(III) with C4 and C6  
670 Dicarboxylic Acids, *Environ. Sci. Technol.*, 51, 9700-9708, 10.1021/acs.est.7b01826, 2017.
- 671 Updyke, K. M., Nguyen, T. B., and Nizkorodov, S. A.: Formation of brown carbon via reactions of ammonia with  
672 secondary organic aerosols from biogenic and anthropogenic precursors, *Atmos. Environ.*, 63, 22-31,  
673 <https://doi.org/10.1016/j.atmosenv.2012.09.012>, 2012.
- 674 van Donkelaar, A., Martin, R. V., Brauer, M., Kahn, R., Levy, R., Verduzco, C., and Villeneuve, P. J.: Global  
675 Estimates of Ambient Fine Particulate Matter Concentrations from Satellite-Based Aerosol Optical Depth:  
676 Development and Application, *Environmental Health Perspectives*, 118, 847-855, 10.1289/ehp.0901623, 2010.
- 677 Wang, G. H., Zhang, R. Y., Gomez, M. E., Yang, L. X., Zamora, M. L., Hu, M., Lin, Y., Peng, J. F., Guo, S., Meng,  
678 J. J., Li, J. J., Cheng, C. L., Hu, T. F., Ren, Y. Q., Wang, Y. S., Gao, J., Cao, J. J., An, Z. S., Zhou, W. J., Li, G.  
679 H., Wang, J. Y., Tian, P. F., Marrero-Ortiz, W., Secrest, J., Du, Z. F., Zheng, J., Shang, D. J., Zeng, L. M., Shao,  
680 M., Wang, W. G., Huang, Y., Wang, Y., Zhu, Y. J., Li, Y. X., Hu, J. X., Pan, B., Cai, L., Cheng, Y. T., Ji, Y. M.,  
681 Zhang, F., Rosenfeld, D., Liss, P. S., Duce, R. A., Kolb, C. E., and Molina, M. J.: Persistent sulfate formation  
682 from London Fog to Chinese haze, *Proceedings of the National Academy of Sciences of the United States of*



- 683 America, 113, 13630-13635, 10.1073/pnas.1616540113, 2016.
- 684 Washenfelder, R. A., Attwood, A. R., Brock, C. A., Guo, H., Xu, L., Weber, R. J., Ng, N. L., Allen, H. M., Ayres, B.  
685 R., Baumann, K., Cohen, R. C., Draper, D. C., Duffey, K. C., Edgerton, E., Fry, J. L., Hu, W. W., Jimenez, J. L.,  
686 Palm, B. B., Romer, P., Stone, E. A., Wooldridge, P. J., and Brown, S. S.: Biomass burning dominates brown  
687 carbon absorption in the rural southeastern United States, *Geophysical Research Letters*, 42, 653-664,  
688 doi:10.1002/2014GL062444, 2015.
- 689 Wu, C.: Seasonal variation of atmospheric acidic and basic species and the characteristics of gas-particle partition in  
690 a typical city of Guanzhong Basin (in Chinese), Ph. D. The University of Chinese Academy of Sciences, The  
691 University of Chinese Academy of Sciences, Xi'an, 2018.
- 692 Wu, C., Wang, G., Wang, J., Li, J., Ren, Y., Zhang, L., Cao, C., Li, J., Ge, S., Xie, Y., Wang, X., and Xue, G.:  
693 Chemical characteristics of haze particles in Xi'an during Chinese Spring Festival: Impact of fireworks burning,  
694 *Journal of Environmental Sciences*, 71, 179-187, <https://doi.org/10.1016/j.jes.2018.04.008>, 2018.
- 695 Wu, G., Ram, K., Fu, P., Wang, W., Zhang, Y., Liu, X., Stone, E. A., Pradhan, B. B., Dangol, P. M., Panday, A. K.,  
696 Wan, X., Bai, Z., Kang, S., Zhang, Q., and Cong, Z.: Water-Soluble Brown Carbon in Atmospheric Aerosols  
697 from Godavari (Nepal), a Regional Representative of South Asia, *Environ. Sci. Technol.*, 53, 3471-3479,  
698 10.1021/acs.est.9b00596, 2019.
- 699 Xie, M., Chen, X., Hays, M. D., and Holder, A. L.: Composition and light absorption of N-containing aromatic  
700 compounds in organic aerosols from laboratory biomass burning, *Atmos. Chem. Phys.*, 19, 2899-2915,  
701 10.5194/acp-19-2899-2019, 2019.
- 702 Xu, J., Cui, T. Q., Fowler, B., Fankhauser, A., Yang, K., Surratt, J. D., and McNeill, V. F.: Aerosol Brown Carbon  
703 from Dark Reactions of Syringol in Aqueous Aerosol Mimics, *Acs Earth and Space Chemistry*, 2, 608-617,  
704 10.1021/acsearthspacechem.8b00010, 2018.
- 705 Yan, C., Zheng, M., Sullivan, A. P., Bosch, C., Desyaterik, Y., Andersson, A., Li, X., Guo, X., Zhou, T., Gustafsson,  
706 Ö., and Collett, J. L.: Chemical characteristics and light-absorbing property of water-soluble organic carbon in  
707 Beijing: Biomass burning contributions, *Atmos. Environ.*, 121, 4-12,  
708 <https://doi.org/10.1016/j.atmosenv.2015.05.005>, 2015.
- 709 Yan, C. Q., Zheng, M., Bosch, C., Andersson, A., Desyaterik, Y., Sullivan, A. P., Collett, J. L., Zhao, B., Wang, S.  
710 X., He, K. B., and Gustafsson, O.: Important fossil source contribution to brown carbon in Beijing during  
711 winter, *Scientific reports*, 7, DOI: 10.1038/srep43182, 10.1038/srep43182, 2017.
- 712 Yu, L., Smith, J., Laskin, A., Anastasio, C., Laskin, J., and Zhang, Q.: Chemical characterization of SOA formed  
713 from aqueous-phase reactions of phenols with the triplet excited state of carbonyl and hydroxyl radical, *Atmos.*  
714 *Chem. Phys.*, 14, 13801-13816, 10.5194/acp-14-13801-2014, 2014.
- 715 Zhang, X., Lin, Y.-H., Surratt, J. D., and Weber, R. J.: Sources, Composition and Absorption Ångström Exponent of  
716 Light-absorbing Organic Components in Aerosol Extracts from the Los Angeles Basin, *Environ. Sci. Technol.*,  
717 47, 3685-3693, 10.1021/es305047b, 2013.
- 718 Zhao, R., Lee, A. K. Y., Huang, L., Li, X., Yang, F., and Abbatt, J. P. D.: Photochemical processing of aqueous  
719 atmospheric brown carbon, *Atmos. Chem. Phys.*, 15, 6087-6100, 10.5194/acp-15-6087-2015, 2015.
- 720



721 Table 1 Average ( $\pm 1\sigma$ ) values Abs<sub>365</sub>, MAC<sub>365</sub>, and AAE of WS-BrC and WI-BrC, as well as concentrations of  
 722 OC, WSOC, WIOC, and measured organic species in the PM<sub>2.5</sub> aerosols from the rural site of Guanzhong Basin.

	Summer			Winter		
	Average	Daytime	Nighttime	Average	Daytime	Nighttime
Abs <sub>365,WS-BrC</sub> (Mm <sup>-1</sup> )	5.00±1.28	5.64±1.34	4.37±0.83	19.6±8.3	19.2±6.8	19.9±9.5
Abs <sub>365,WI-BrC</sub> (Mm <sup>-1</sup> )	2.95±1.94	4.23±1.93	1.67±0.72	21.9±13.5	17.2±8.2	26.7±15.8
MAC <sub>365,WS-BrC</sub> (m <sup>2</sup> g <sup>-1</sup> )	1.00±0.18	0.99±0.17	1.01±0.18	0.93±0.25	0.92±0.21	0.94±0.28
MAC <sub>365,WI-BrC</sub> (m <sup>2</sup> g <sup>-1</sup> )	1.82±1.06	2.45±1.14	1.18±0.36	0.95±0.32	0.85±0.34	1.05±0.28
AAE <sub>WS-BrC</sub>	5.43±0.41	5.56±0.4	5.30±0.38	5.11±0.53	5.14±0.2	5.07±0.72
AAE <sub>WI-BrC</sub>	5.01±0.58	4.74±0.19	5.28±0.71	6.04±0.22	5.94±0.12	6.15±0.24
OC (µg m <sup>-3</sup> )	6.78±1.77	7.74±1.73	5.83±1.19	45.9±22.9	44.0±17.2	47.9±27.2
WSOC (µg m <sup>-3</sup> )	5.06±1.11	5.72±1.02	4.39±0.72	21.9±9.3	22.1±8.0	21.7±10.4
WIOC (µg m <sup>-3</sup> )	1.73±0.87	2.02±1.04	1.44±0.53	24.0±14.3	21.9±10.1	26.2±17.3
WSOC/OC	0.75±0.07	0.75±0.09	0.76±0.04	0.50±0.09	0.51±0.08	0.48±0.10
Parent-PAHs (ng m <sup>-3</sup> )	8.81±5.09	11.6±5.7	5.98±1.9	82.3±53.7	70.8±35.4	93.9±65.1
OPAHs (ng m <sup>-3</sup> )	14.0±14.0	23.0±15.1	4.97±1.34	98.3±59.5	89.4±39.8	107±73
Nitrophenols (ng m <sup>-3</sup> )	0.94±0.26	0.87±0.26	1.02±0.24	72.6±63.7	41.1±15.5	104±77
SOA <sub>i</sub> <sup>a</sup> (ng m <sup>-3</sup> )	18.6±9.7	15.0±8.0	22.1±9.8	BDL <sup>c</sup>	BDL	BDL
SOA <sub>p</sub> <sup>b</sup> (ng m <sup>-3</sup> )	22.0±6.7	25.2±6.7	18.9±5.0	BDL	BDL	BDL
Levogluconan (ng m <sup>-3</sup> )	98.7±83.7	142±89	55.1±48.7	601±301	569±138	633±401

723 <sup>a</sup> SOA<sub>i</sub>: Tracers of SOA formed from isoprene (SOA<sub>i</sub>) oxidation, i.e., the sum of 2-methylglyceric acid, 2-methylthreitol, and 2-  
 724 methylerythritol.

725 <sup>b</sup> SOA<sub>p</sub>: Tracers of SOA formed from  $\alpha$ - $\beta$ -pinene (SOA<sub>p</sub>) oxidation, i.e., the sum of pinonic acid, pinic acid, and 3-methyl-1,2,3-  
 726 butanetricarboxylic acid.

727 <sup>c</sup> BDL: below detection limit (<0.17 ng m<sup>-3</sup>).

728

729

730 Table 2 Comparison of MAC<sub>365,WS-BrC</sub> in the present study and those reported in earlier studies in China, India, and  
 731 the United States (US).

Sampling site	Sampling time	Season	MAC <sub>365,WS-BrC</sub> (m <sup>2</sup> g <sup>-1</sup> )	Reference
Lincun, Shaanxi, China	Aug. 3-23, 2016	Summer	1.00±0.18	This study
	Jan. 20-Feb 1, 2017	Winter	0.93±0.25	
Xi'an, China	Jun. 1-Aug. 31, 2009	Summer	0.98 ± 0.21	Huang et al. (2018)
	Nov.15, 2008-Mar. 14, 2009	Winter	1.65 ± 0.36	
Beijing, China	Jun. 20-Jul. 20, 2009	Summer	1.8 ± 0.2	Cheng et al. (2011)
	Jan.9-Feb. 12, 2009	Winter	0.7 ± 0.2	
Seoul, Korea	Aug. 13-Sep. 9, 2013	Summer	0.28	Kim et al. (2016)
	Jan. 9-Feb 8, 2013	Winter	1.02	
New Delhi, India	Oct. 24, 2010-Mar. 25, 2011	Winter	1.6 ± 0.5	Kirillova et al. (2014b)
Los Angeles Basin, US	mid-May - mid-June, 2010	summer	0.71	Zhang et al. (2013)
Southeastern US	2007	annually	0.3–0.7	Hecobian et al. (2010)
Atlanta, US	May 17-Sep. 29, 2012	summer and fall	0.14-0.53	Liu et al. (2013)



732

733

734

735

736 Table 3 Average direct solar absorption of water-soluble and water-insoluble BrC during summer and winter

	WSOC		WIOC	
	Summer	Winter	Summer	Winter
<i>Actinic flux (<math>\times 10^{14}</math> quanta <math>s^{-1} cm^{-2}</math>)</i>				
300-400 nm	1.55±0.43	2.14±0.92	1.03±0.64	2.53±1.52
400-700 nm	1.77±0.6	2.67±1.04	1.24±0.8	2.58±1.48
<i>Irradiance (<math>W m^{-2}</math>)</i>				
300-400 nm	0.51±0.14	0.57±0.25	0.34±0.21	0.68±0.41
400-700 nm	0.49±0.17	0.57±0.22	0.35±0.23	0.55±0.32
<i>Relative to EC (%)</i>				
300-400 nm	49.4±14.5	25.9±5.47	29.4±11.0	29.0±10.4
400-700 nm	10.0±3.52	4.99±1.23	6.19±2.42	4.51±1.44

737

738



739

### Figure Caption

740 Figure 1 Temporal variation of meteorological parameters (a and b), concentrations of major  
741 chemical compositions,  $Abs_{365}$ ,  $MAC_{365}$ , and AAE of water-soluble and water-insoluble  
742 BrC in  $PM_{2.5}$  from the rural area of Northwest China.

743

744 Figure 2 Average spectra of absorption coefficient ( $Abs_{\lambda}$ ) (a,b) and mass absorption coefficient  
745 ( $MAC_{\lambda}$ ) (c,d) of water-soluble (WS-BrC) and water-insoluble (WI-BrC) BrC, as well as the  
746 ratio of  $MAC_{\lambda, WI-BrC}$  to  $MAC_{\lambda, WS-BrC}$  (e,f) during daytime and nighttime of summer and  
747 winter. Absorption Ångström exponent (AAE) is calculated by a linear regression of log  
748  $Abs_{\lambda}$  versus log  $\lambda$  in the wavelength range of 300–450 nm.

749

750 Figure 3 Cross correlations between  $Abs_{365, WS-BrC}$ ,  $Abs_{365, WI-BrC}$ , selected chemical compositions,  
751 and RH in summer. The numbers at the upper right denote the linear correlation coefficients  
752 ( $r^2$ ) of the corresponding scatter plots.

753

754 Figure 4 Cross correlations between  $Abs_{365, WS-BrC}$ ,  $Abs_{365, WI-BrC}$ , selected chemical compositions,  
755 and RH in winter. The numbers at the upper right denote the linear correlation coefficients  
756 ( $r^2$ ) of the corresponding scatter plots.

757

758 Figure 5 Average contribution of parent-PAHs and OPAHs to the bulk light absorption of WI-  
759 BrC (300–700 nm) during daytime and nighttime of summer and winter.

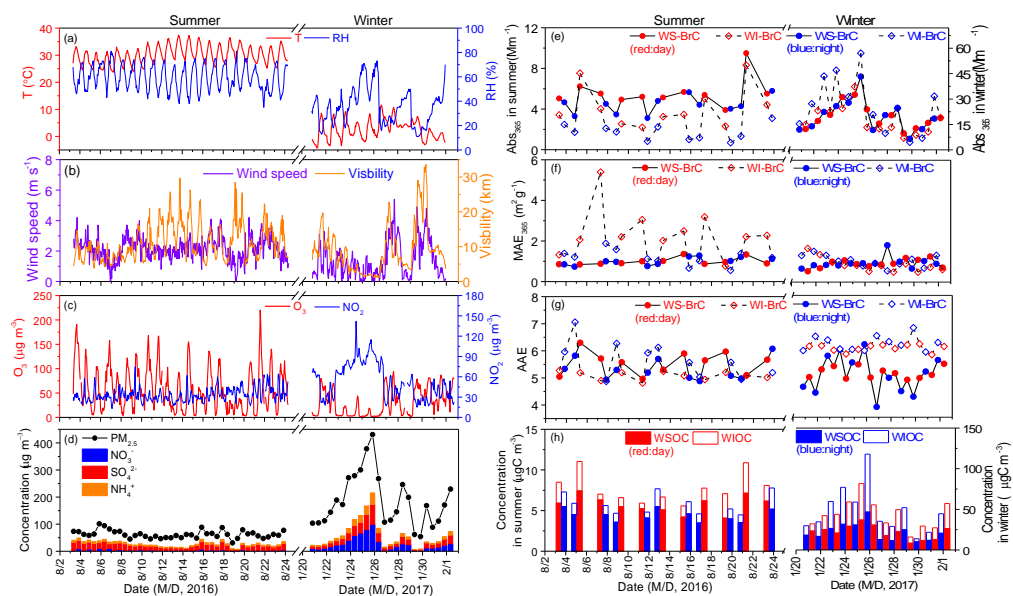
760

761

762



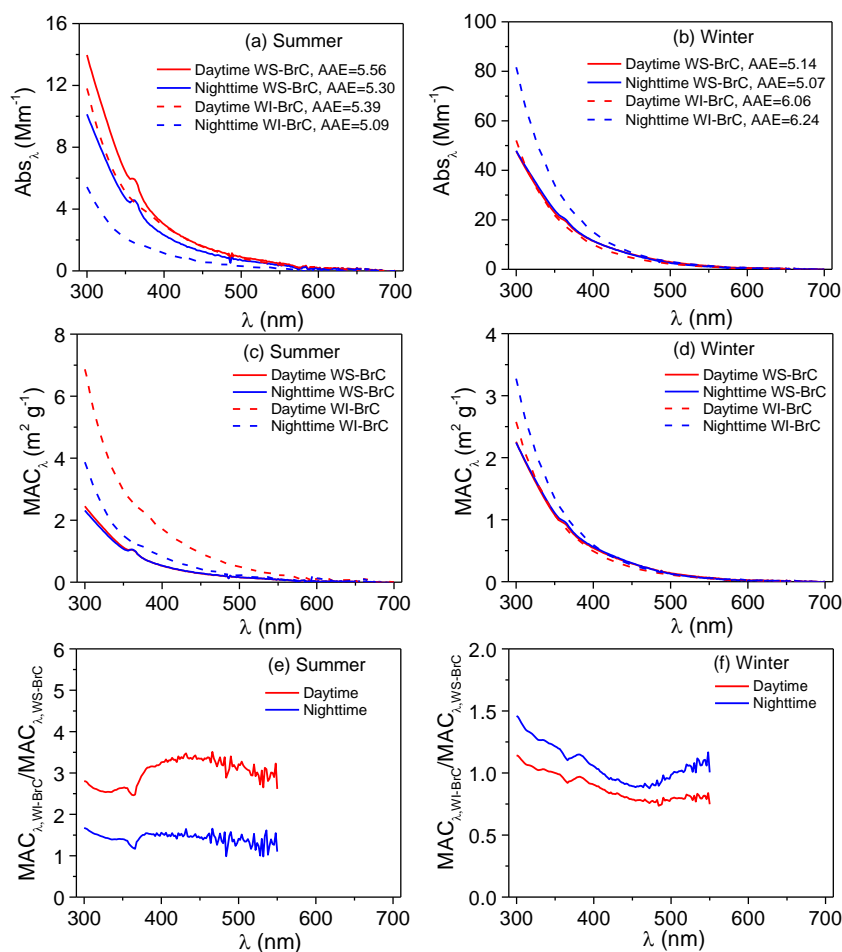
763



764

765 Figure 1 Temporal variation of meteorological parameters (a and b), concentrations of major chemical  
766 compositions, Abs<sub>365</sub>, MAC<sub>365</sub>, and AAE of water-soluble and water-insoluble BrC in PM<sub>2.5</sub> from the rural  
767 area of Northwest China.

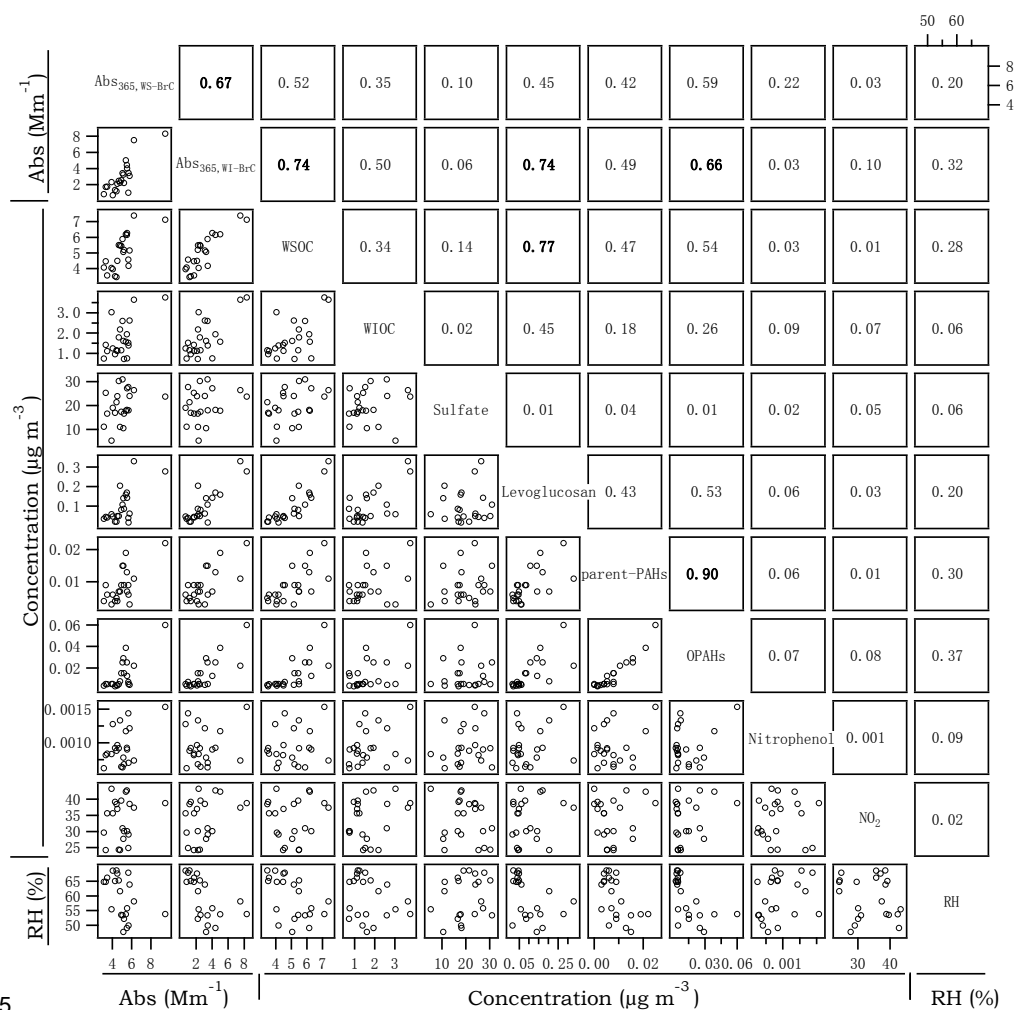
768



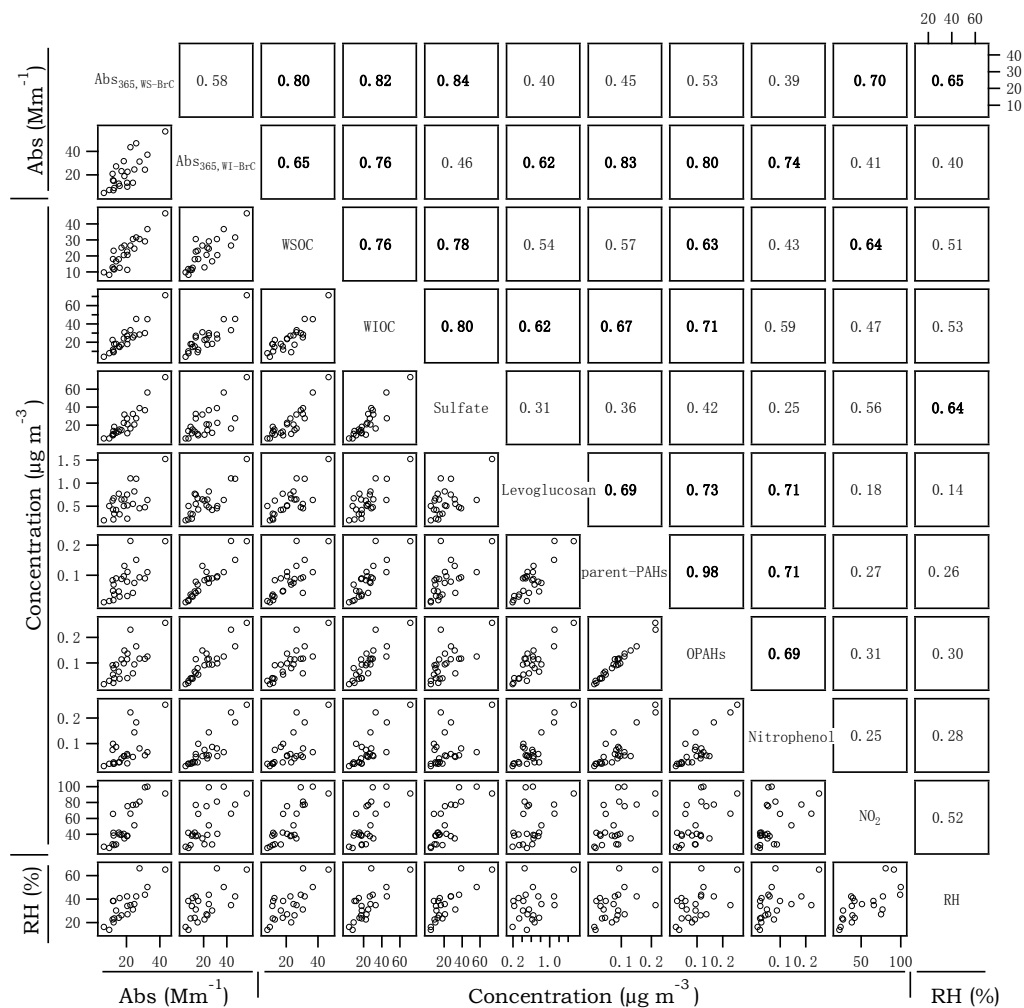
769

770 Figure 2 Average spectra of absorption coefficient ( $Abs_{\lambda}$ ) (a,b) and mass absorption coefficient ( $MAC_{\lambda}$ ) (c,d)  
771 of water-soluble (WS-BrC) and water-insoluble (WI-BrC) BrC, as well as the ratio of  $MAC_{\lambda,WI-BrC}$  to  $MAC_{\lambda,WS-BrC}$   
772 BrC (e,f) during daytime and nighttime of summer and winter. Absorption Ångström exponent (AAE) is  
773 calculated by a linear regression of  $\log Abs_{\lambda}$  versus  $\log \lambda$  in the wavelength range of 300–450 nm.  
774



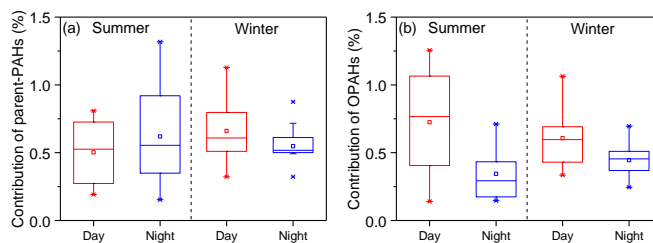


775  
 776 Figure 3 Cross-correlations between Abs<sub>365,WS-BrC</sub>, Abs<sub>365,WI-BrC</sub>, selected chemical components, and RH in  
 777 summer. The numbers at the upper right denote the linear correlation coefficients (r<sup>2</sup>) of the corresponding  
 778 scatter plots.  
 779



780  
 781 Figure 4 Cross-correlations between Abs<sub>365,WS-BrC</sub>, Abs<sub>365,WI-BrC</sub>, selected chemical components, and RH in  
 782 winter. The numbers at the upper right denote the linear correlation coefficients ( $r^2$ ) of the corresponding  
 783 scatter plots.

784



785

786 Figure 5 Average contribution of parent-PAHs and OPAHs to the bulk light absorption of WI-BrC (300–700  
787 nm) during daytime and nighttime of summer and winter.

788

789